Tunneling magnetoresistance based on a Cr/graphene/Cr magnetotunnel junction*

Luan Gui-Ping(栾桂苹)[a], Zhang Pei-Ran(张沛然)[a], Jiao Na(焦 娜)[a], and Sun Li-Zhong(孙立忠)[b]†

[a] Department of Physics, Xiangtan University, Xiangtan 411105, China
[b] Hunan Provincial Key Laboratory of Thin Film Materials and Devices, School of Materials Science and Engineering, Xiangtan University, Xiangtan 411105, China

(Received 16 January 2015; revised manuscript received 27 April 2015; published online 9 October 2015)

Using the density functional theory and the nonequilibrium Green's function method, we studied the finite-bias quantum transport in a Cr/graphene/Cr magnetotunnel junction (MTJ) constructed by a single graphene layer sandwiched between two semi-infinite Cr(111) electrodes. We found that the tunneling magnetoresistance (TMR) ratio in this MTJ reached 108%, which is close to that of a perfect spin filter. Under an external positive bias, we found that the TMR ratio remained constant at 65%, in contrast to MgO-based MTJs, the TMR ratios of which decrease with increasing bias. These results indicate that the Cr/graphene/Cr MTJ is a promising candidate for spintronics applications.

Keywords: graphene, first-principles method, magnetotunnel junction, tunneling magnetoresistance

PACS: 72.15.Gd, 72.25.Mk **DOI:** 10.1088/1674-1056/24/11/117201

1. Introduction

Spintronics is a promising next-generation electronic technology based on manipulating the spin degrees of freedom. In comparison with the traditional electronic devices, those based on spintronics have advantages of low power consumption, fast response, and high storage density. Recently, prototype spintronics devices have been realized, such as a magnetic read head and memory-storage unit. One of the most important topics in spintronics is how to obtain high spin-polarized electron currents.[1,2] The magnetotunnel junction (MTJ) is a basic physical model for this type of spin-filtering effect. Numerous experimental[3–6] and theoretical[7–9] studies have focused on the spin-polarized tunneling properties of MTJs. In general, the spin-filter effect of MTJs is achieved by the spin-dependent electron transmission through the interface between the insulator (or semiconductor) and the ferromagnetic metals.[10] The tunneling magnetoresistance (TMR) ratio is the most important parameter that determines the performance of MTJs.[11] It is therefore crucial to achieve a high TMR ratio for practical applications of MTJs. One of the main challenges in obtaining a high TMR ratio is achieving a well-ordered interface in the MTJ.[11–13] Recently, both theoretical and experimental results[8,14,15] have shown that by using graphene or h-BN sheets as the spacer in MTJs, high TMR ratios can be achieved.

Graphene, a single layer of carbon atoms in a honeycomb lattice, has attracted immense interest during the last decade because of its remarkable properties, such as high electron mobility,[16,17] quantum Hall effect,[18–21] high thermal conductivity,[22,23] and long-distance scattering.[24] As a next-generation, non-silicon, micro-electronic material, graphene also shows a great potential for spintronics applications.[25–27] Large-area and exceptionally high-quality epitaxial graphene layers can be grown on transition metal (TM) substrates.[28–31] Theoretical studies have shown that graphene retains a relatively well-integrated lattice structure and a perfect interface with TM substrates owing to its strong in-plane sp^2 hybridization.[32,33] Moreover, its electronic transport perpendicular to the plane shows strong selectivity near the high-symmetry K (K') point in the reciprocal space, which makes graphene a good tunneling barrier and spin-selective insulator in MTJs. Recently, much effort has been devoted to MTJs constructed with graphene and 3d TMs Ni(111) and Co(111) because of the close match in the lattice constants of graphene and these metals. For example, Karpan *et al.*[8,14] reported that MTJs based on multilayer graphene and Ni or Co electrodes show perfect spin-filter effects. However, multilayer graphene has a very wide potential barrier, which increases scattering of transport electrons and greatly reduces the efficiency of the device. Therefore, finding suitable 3d TM electrodes that improve the spin-filter effect of the MTJs based on monolayer graphene is crucial for the application of graphene in spintronics devices.

In this study, we investigate the magnetism of a Cr/graphene/Cr MTJ by calculating the local density of states (LDOS) and $k_{||}$-resolved transmission conductance at zero

*Project supported by the National Natural Science Foundation of China (Grant Nos. 10874143, 10974166, and 11574260), the Program for New Century Excellent Talents in University, China (Grant No. NCET-10-0169), the National Innovation Foundation for Graduate, China (Grant No. 201310530003), and the Computational Support from Shanghai Super-computer Center, China.

†Corresponding author. E-mail: lzsun@xtu.edu.cn

© 2015 Chinese Physical Society and IOP Publishing Ltd

bias. Importantly, the TMR ratio of the sandwich structure exceeds 100% and is close to that of a perfect spin filter. Moreover, a stable TMR ratio of Cr/graphene/Cr under an external bias is observed, demonstrating its potential in spintronics devices.

2. Models and computational details

The most favorable configuration for graphene/Cr(111) is a $\sqrt{3}\times\sqrt{3}$ graphene supercell matching the 1×1 Cr metal cell as shown in Figs. 1(a) and 1(b). The lattice mismatch of the graphene and Cr(111) surfaces in the planar junction is less than 3%. We constructed the MTJ from two semi-infinite Cr(111) electrodes and monolayer graphene as shown in Fig. 1(c). In Figs. 1(a) and 1(b), the blue, pink, yellow, and orange spheres represent the carbon atoms on hollow (C_4, C_5, C_6), top (C_1), hcp (C_2), and fcc (C_3) sites, respectively. It can be seen that the C_1 atom adsorbs on the top site of the left metal electrode, but on the hcp site of the right metal electrode. However, the C_2 atom adsorbs on the top site of the right metal electrode, but on the hcp site of the left metal electrode. The C_3 adsorbs on the fcc sites of both electrodes. The C_4, C_5, and C_6 atoms adsorb on the hollow sites of both electrodes. According to the sites of the carbon atoms, there are four non-equivalent types of carbon atoms in the spacer, namely, C_1, C_2, C_3, and (C_4, C_5, C_6), which breaks the inversion symmetry of the MTJ. The asymmetric feature of the MTJ will induce asymmetric transport properties. To obtain the stable structures of the MTJ, the atomic coordinates were optimized using the Vienna *ab initio* simulation package based on the density functional theory. The total energy converges to 10^{-5} eV and the atoms of the system are fully relaxed until the residual force is less than 0.01 eV/Å. The Perdew–Burke–Ernzerhof parameterized spin-polarized generalized gradient approximation[34,35] was used to describe the exchange–correlation functional. The quantum transport calculations were carried out with the real-space nonequilibrium Green's function method implemented in the Atomistix Toolkit package. It has been demonstrated that this method can effectively describe the TMR effect of MTJs with planar contacts (e.g., Fe/MgO/Fe) and the electronic properties of the TM.[36] In the electronic transport calculations, the Brillouin zone was sampled using a $20\times20\times100$ k-point grid, and the charge density and potentials were determined on a real-space grid with a mesh cutoff energy of 300 Ry. The total energy convergence was set at 10^{-5} Ry. All computational parameters used in the present study were optimized. The TMR ratio is defined as TMR = $(G_{\rm P}-G_{\rm AP})/G_{\rm AP}\times100\% = (G_{\uparrow\uparrow}+G_{\downarrow\downarrow}-2G_{\uparrow\downarrow})/2G_{\uparrow\downarrow}\times100\%$, where $G_{\uparrow\uparrow}$ and $G_{\downarrow\downarrow}$ are the majority and the minority spin-resolved transmission conductances, respectively, when the magnetic configuration of the two Cr electrodes is parallel (P); and $G_{\uparrow\downarrow}$ is the spin-resolved transmission conductance when the magnetic configuration of the two Cr electrodes is anti-parallel (AP).

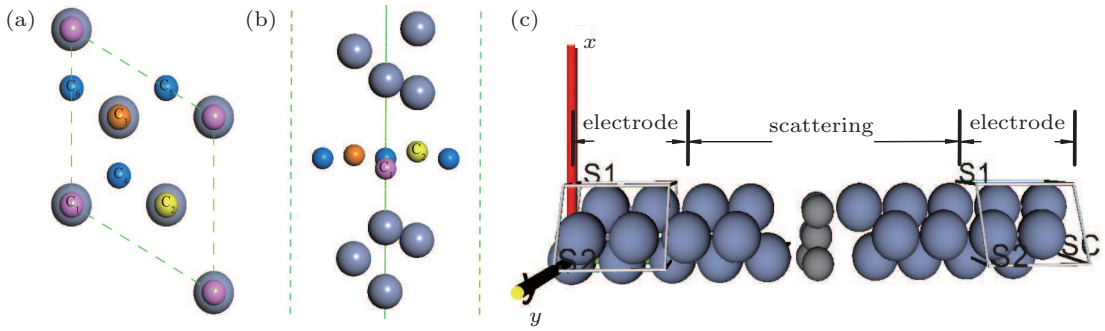


Fig. 1. (color online) (a) Top view of the graphene/Cr(111) planar junction (the large spheres represent the Cr atoms and the small spheres represent the C atoms). (b) Side view of the Cr/graphene/Cr junction; the nearest C–Cr distance is 2.22 Å after optimization. (c) Two-probe system of Cr/graphene/Cr; the blue and black represent the Cr and C atoms, respectively.

3. Results and discussion

The spin transmission spectra of the Cr/graphene/Cr MTJ under equilibrium conditions (zero bias) are presented in Fig. 2. For the P configuration, the spin states split around the Fermi level $E_{\rm F}$, and the transmission coefficient of the spin-up channel is much larger than that of the spin-down channel. In contrast, for the AP configuration, both spin channels display similar transmission coefficients at $E_{\rm F}$. The transmission coefficients of the AP configuration are similar to those of the lower transmission channel of the P configuration; this result is similar to that reported for Ni/graphene$_n$/Ni.[14] Furthermore, we calculated the TMR ratio of the Cr/graphene/Cr MTJ to be approximately 108%, which far exceeds the values reported for Ni/graphene/Ni (17%) and Co/graphene/Co (60%) MTJs.[37] Considering the different computational methods used, we recalculated the TMR ratio of Ni/graphene/Ni to be 42%, which is still significantly lower than that of Cr/graphene/Cr. Thus, the Cr electrode is more favorable for graphene-based MTJs.

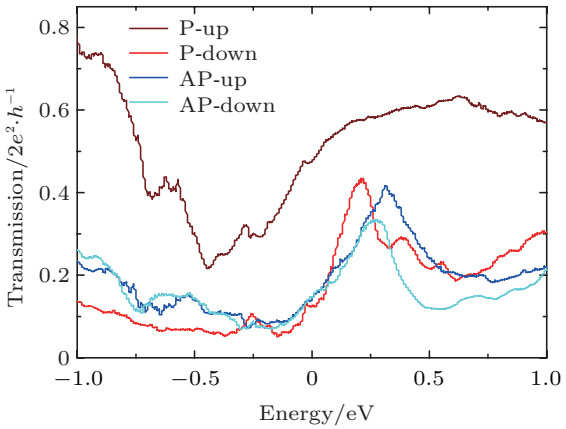


Fig. 2. (color online) Spin transmission spectra for the P and AP configurations of the Cr/graphene/Cr MTJ under zero bias. The Fermi level (E_F) is set to zero.

To understand the transport properties of the Cr/graphene/Cr MTJ under zero bias, we calculated the LDOS in the real space of the system at E_F as shown in Fig. 3. The LDOS can clearly show the electron transport channels of a device in real space. For the P configuration, the LDOS of the spin-up channel is well distributed through the MTJ, whereas that of the spin-down channel is localized on the Cr electrodes, in particular, around the atoms close to graphene. The localization of the spin-down channel means that the effective transport channel mainly comes from the spin-up states. The blockage of the spin-down channel induced by the localization of the LDOS results in the transmission coefficient of the spin-up channel exceeding that of the spin-down channel. For the AP configuration, the LDOS is evenly distributed on graphene; the LDOS is only well distributed on one of the electrodes. Such quasi-localization in the AP configuration of both transport channels decreases the transmission coefficients. These results demonstrate that only the spin-up state of the P configuration can provide an effective transmission channel for the spin-polarized system.

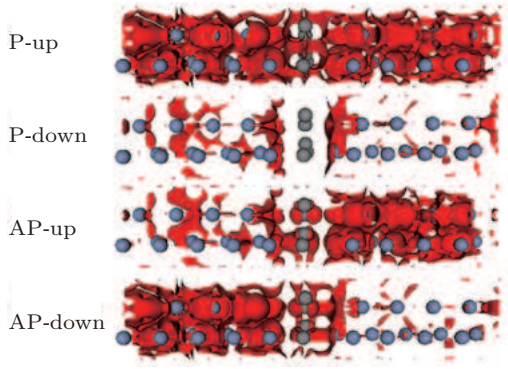


Fig. 3. (color online) LDOS of the Cr/graphene/Cr MTJ in P and AP configurations under zero bias.

To explain the high TMR ratio of the system, we calculated the $k_{||}$-resolved transmission conductance and band structures, the results are shown in Fig. 4. The band structure shown in Fig. 4(b) indicates that the free-standing graphene is a semi-metal with its band structure linearly dispersed around E_F. The π and π^* bands intersect at the K point in the Brillouin zone. The band structure of graphene with a $\sqrt{3} \times \sqrt{3}$ supercell, as shown in Fig. 4(c), indicates that the K point is back-folded to the Γ (G) point. The band structures of the Cr/graphene/Cr MTJ are shown in Fig. 4(d). The interaction between the graphene sheet and Cr produces a bandgap for graphene of about 0.03 eV. In addition, the graphene is n-type doped by the electrodes. The results in Fig. 4(d) indicate that the electronic transport of the system occurs around the high-symmetry M and K points in reciprocal space because of the overlap of the band structures derived from graphene and the Cr electrodes at these k-points. For the MTJ, because there is spin-up transmission in the Cr(111) system around the G, M, and K points, as shown in Fig. 4(a), in the P configuration of the Cr/graphene/Cr MTJ, there is high $k_{||}$-resolved spin-up transmission conductance around the M and K points owing to the selection rules. Such selection rules can be directly evaluated from the $k_{||}$-resolved transmission conductance because this is the integral of the wave function at the Fermi surface projections.[38] The $k_{||}$-resolved transmission conductance reflects the ability of the wave functions to penetrate from the left electrode to the right electrode at some specific k-points. In other words, the more compatible the wave functions on both sides of the interface, the larger the $k_{||}$-resolved transmission conductance. Although there is high spin-down transmission around the G and K points of the Cr electrodes along the (111) direction, the $k_{||}$-resolved transmission conductance for the spin-down state in the P configuration is low at the G, M, and K points because of the selection rules; that is, because of the incompatibility of the wave functions on both sides of the interface.[38] The $k_{||}$-resolved transmission conductance for the AP configuration is mainly determined by the overlap between the spin-up and spin-down states of the two opposite sides of the junction. Consequently, the $k_{||}$-resolved transmission conductance of the AP configuration is lower at the G, M, and K points. It is these characteristics of the $k_{||}$-resolved transmission conductance that are directly responsible for the high TMR ratio. Moreover, an asymmetric $k_{||}$-resolved transmission conductance occurs for both spin channels in the AP configuration because of the asymmetric nature of the MTJ. The influence of the structural properties on the spin polarization can be determined from the Mulliken population of carbon atoms in the MTJ. For example, for the AP configuration under zero bias, the Mulliken population of carbon atoms shown in Table 1 indicates that there are four types of carbon atoms in the MTJ, which is in agreement with the four types of atom sites mentioned above. The asymmetric MTJ will produce different responses for the spin-up and spin-down states, which further contributes to the asymmetric Fermi surface projections for the two spin channels.

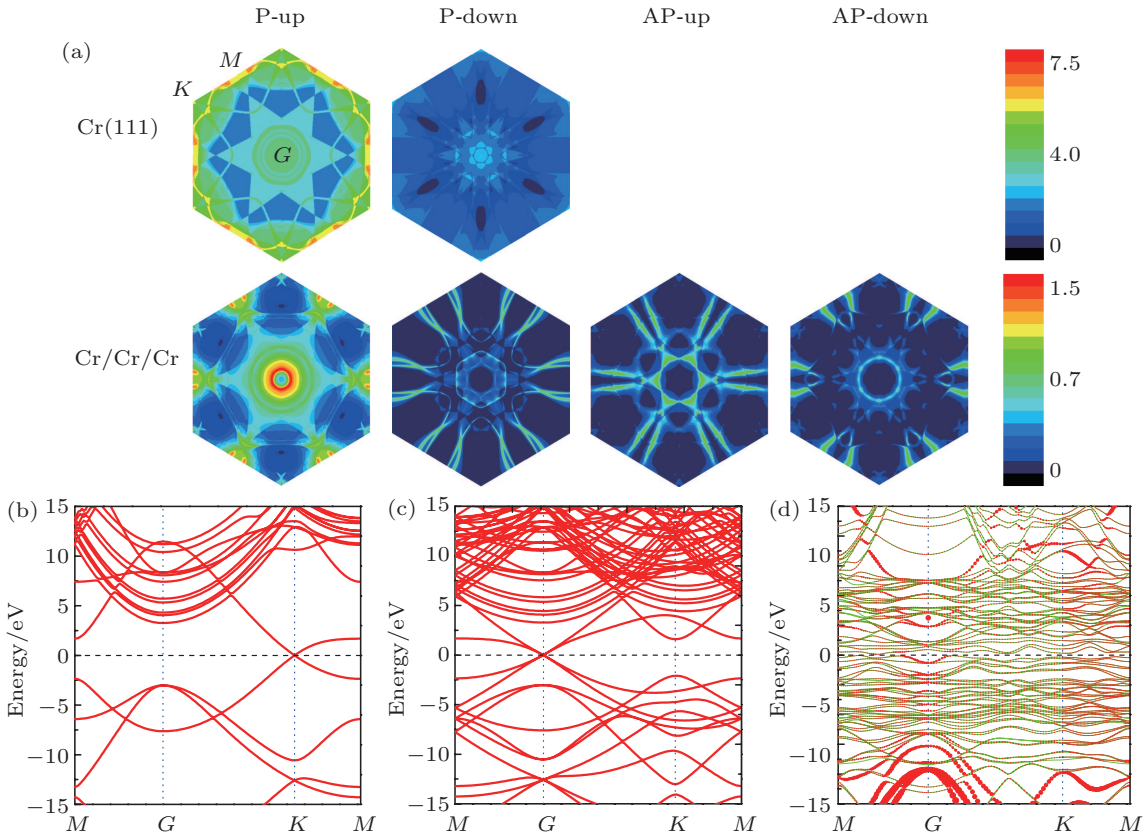


Fig. 4. (color online) (a) The $k_{||}$-resolved transmission conductance through bulk Cr along the (111) direction and through the Cr/graphene/Cr MTJ. (b), (c) Band structures of graphene with a 1×1 unit cell and a $\sqrt{3} \times \sqrt{3}$ supercell, respectively. (d) Band structure of the Cr/graphene/Cr MTJ; the red dots represent the contribution of the carbon states to the band derived from the projection of the wave function to the specific band according to different k points. The size of the red dots denotes the relative magnitude of the contribution of the carbon states to different k points. The projected density of state of graphene onto the total bands. The Fermi level is set to zero and the high-symmetry points are $G = (0,0,0)$, $K = (-1/3,2/3,0)$, and $M = (0,1/2,0)$.

Table 1. Mulliken population of C atoms in a Cr/graphene/Cr MTJ under biases of 0.5 V, 0.0 V, and −0.5 V. The subscripted number is the sequence of C in the interfacial layer between graphene and the Cr electrode.

Bias	State	C_1	C_2	C_3	C_4	C_5	C_6	Sum
0.5 V	AP-up	2.03	1.98	2.02	2.08	2.08	2.08	12.27
	AP-down	1.96	2.01	2.01	2.05	2.05	2.05	12.13
0.0 V	AP-up	2.02	1.97	2.02	2.06	2.06	2.06	–
	AP-down	1.97	2.02	2.02	2.06	2.06	2.06	–
−0.5 V	AP-up	1.98	1.94	1.98	2.04	2.14	2.03	12.11
	AP-down	1.95	2.01	1.99	2.07	2.17	2.06	12.25

The *I*–*V* curves were calculated to further evaluate the transport properties of the Cr/graphene/Cr MTJ under an external bias and the results are shown in Fig. 5(a). The spin-up *I*–*V* curve of the P configuration is linear with a notably larger current than that of the spin-down channel of the P configuration and of both channels of the AP configuration. The transmission conductance at the Fermi level under external bias is shown in Fig. 5(b). Our results show that the spin-up transmission of the P configuration is only slightly influenced by the external bias. From the LDOS of the two channels of the P and AP configurations shown in Fig. 3, we can see that only the spin-up channel of the P configuration is in an extended state. The other three channels are localized to different extents. The localized states are more sensitive to the external bias. Such sensitivity can be clearly shown by the dependence of the LDOS on the external bias, as shown in Fig. s1 in the supplementary materials. The transmission of the spin-down channel for the P configuration initially increases and then decreases with increasing bias. The turning points are 0.3 V and −0.4 V for positive and negative biases, respectively. For the AP configuration, the spin-up transmission increases almost linearly with increasing bias. However, the transmission of the spin-down channel has a turning point at around 0.3 V under positive bias. The increase in transmission for the AP configuration under external bias will reduce the TMR ratio of the system. The turning point of the spin-down channel for the AP configuration only occurs under positive bias, which produces an asymmetric dependence of the TMR ratio on the external bias. Such an asymmetric dependence of the TMR ratio on the bias can be seen for the Cr/graphene/Cr MTJ in the inset of Fig. 5(b). The TMR ratio reduces in the bias window of [−0.5 V, 0.2 V], which is similar to the behavior of the Fe/MgO/Fe MTJ reported by Yuasa.[11] When the bias is larger than 0.2 V, the TMR ratio becomes constant, which is similar to the behavior reported previously for Ni/graphene$_5$/Ni[9] and Fe-intercalated

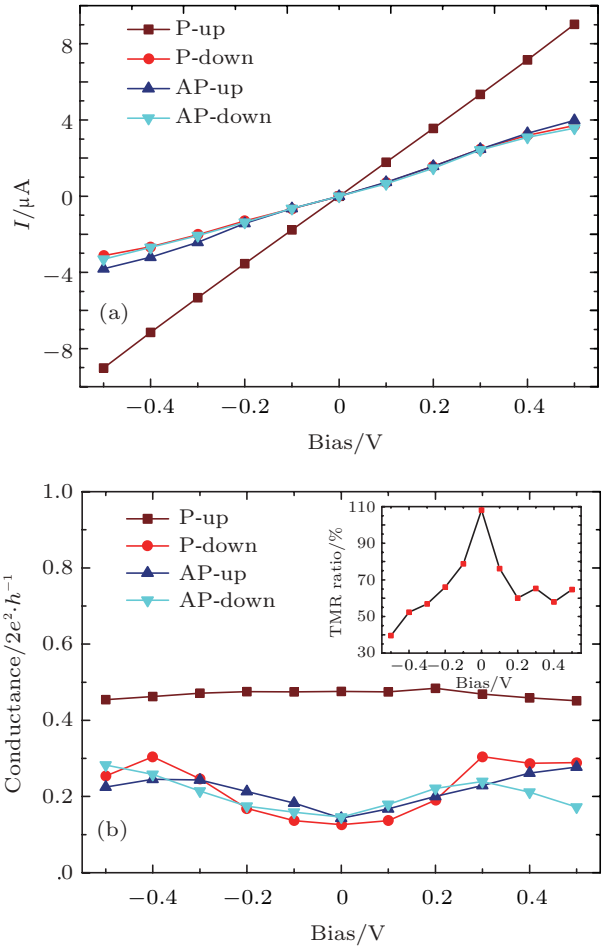


Fig. 5. (color online) (a) The *I*–*V* curves for the P and AP configurations. (b) Bias-dependent transmission curves for the P and AP configurations. Inset: TMR ratio as a function of bias.

bilayer graphene sandwich structure.[39] The bias-dependent asymmetrical characteristics of the TMR ratio result from the asymmetric transmission of the AP configuration, especially the spin-down channel. To further investigate this mechanism, we calculated the Mulliken population of carbon atoms for the AP configuration under 0.5 V and −0.5 V external biases. The results are listed in Table 1 and show that the sum of the spin-up Mulliken population of carbon atoms is larger than that of the spin-down states (12.27 for spin-up and 12.13 for spin-down) under positive bias; however, under negative bias, this trend is reversed (12.11 for spin-up and 12.25 for spin-down). As mentioned above, the structure of the Cr/graphene/Cr MTJ is asymmetric. Moreover, the carbon atoms are in different planes and experience asymmetrical distortion, as shown in Fig. 1(b), meaning that they will have different coupling properties with the two metal electrodes. For the AP configuration, the electron gain and loss will be asymmetric because the spin polarization is different for the two Cr electrodes. This will serve to further induce the asymmetric electron potential between the two interfaces of the spacer. To clearly represent this effect, the spin-resolved total DOS of Cr on the top sites are shown in Fig. 6. The DOS of the spin-up states near the Fermi level is different from that of the spin-down states because of the asymmetric coupling between graphene and the two electrodes. For the AP configuration, if the left electrode is in the spin-up state corresponding to the spin-up channel of the DOS, the right electrode corresponds to the spin-down state of the DOS. The DOS will shift to higher (lower) energy under positive (negative) external bias. The different energy shifts of the DOS will result in different transport responses under positive and negative biases. Consequently, the transmission for the AP configuration has an asymmetric dependence on the external bias.

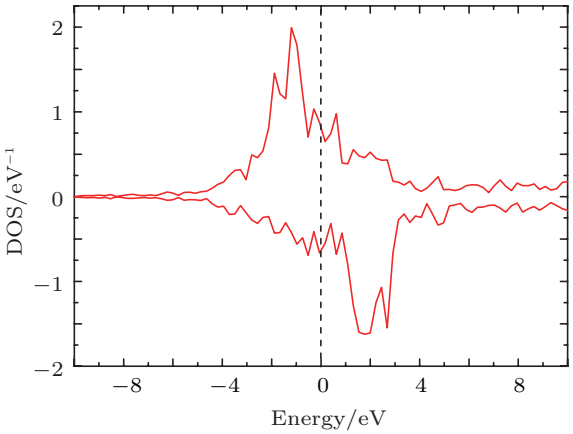


Fig. 6. (color online) Spin-resolved total DOS of Cr on the nearest top-site carbon.

4. Conclusion

We have demonstrated that the TMR ratio of a Cr/graphene/Cr MTJ reaches 108% under zero bias, which is close to that of a perfect spin filter. Moreover, the TMR ratio is dependent on the external bias and decreases with increasing bias in the window of [−0.5 V, 0.2 V]; however, when the bias is larger than 0.2 V, the TMR ratio is constant at 65%. This feature is markedly different from that of the conventional MgO-based MTJs in which the TMR continually decreases with increasing bias. The stable TMR ratio of the Cr/graphene/Cr MTJ under positive external bias demonstrates its potential for spintronics applications.

References

[1] Tsymbal E Y, Burlakov V M and Oleinik I I 2002 *Phys. Rev. B* **66** 073201
[2] Petukhov A G, Chantis A N and Demchenko D O 2002 *Phys. Rev. Lett.* **89** 107205
[3] Ikeda S, Hayakawa J, Ashizawa Y, Lee Y M, Miura K, Hasegawa H, Tsunoda M, Matsukura F and Ohno H 2008 *Appl. Phys. Lett.* **93** 082508
[4] McCreary K M, Swartz A G, Han W, Fabian J and Kawakami R K 2012 *Phys. Rev. Lett.* **109** 186604
[5] Wojtaszek M, Vera-Marun I J, Maassen T and van Wees B J 2013 *Phys. Rev. B* **87** 081402
[6] Ke Y Q, Xia K and Guo H 2010 *Phys. Rev. Lett.* **105** 236801
[7] Hu M L, Yu Z Z, Zhang K W, Sun L Z and Zhong J X 2011 *The Journal of Physical Chemistry C* **115** 8260
[8] Karpan V M, Khomyakov P A, Starikov A A, Giovannetti G, Zwierzycki M, Talanana M, Brocks G, Brink J van den and Kelly P J 2008 *Phys. Rev. B* **78** 195419

[9] Saha K K, Blom A, Thygesen K S and Nikolic B K 2012 *Phys. Rev. B* **85** 184426

[10] Zhu J G and Park C 2006 *Materials Today* **9** 36

[11] Yuasa S, Nagahama T, Fukushima A, Suzuki Y and Ando K 2004 *Nat. Mater.* **3** 868

[12] Heiliger C, Zahn P, Yavorsky B Y and Mertig I 2006 *Phys. Rev. B* **73** 214441

[13] Tanaka C, Nowak J and Moodera J 1997 *J. Appl. Phys.* **81** 5515

[14] Karpan V, Giovannetti G, Khomyakov P, Talanana M, Starikov A, Zwierzycki M, Van Den Brink J, Brocks G and Kelly P 2007 *Phys. Rev. Lett.* **99** 176602

[15] Karpan V M, Khomyakov P A, Giovannetti G, Starikov A A and Kelly P J 2011 *Phys. Rev. B* **84** 153406

[16] Novoselov K S, Geim A K, Morozov S V, Jiang D, Zhang Y, Dubonos S V, Grigorieva I V and Firsov A A 2004 *Science* **306** 666

[17] Abanin D A, Lee P A, and Levitov L S 2006 *Phys. Rev. Lett.* **96** 176803

[18] Zhang Y B, Tan Y W, Stormer H L and Kim P 2005 *Nature* **438** 201

[19] Berger C, Song Z M, Li X B, Wu X S, Brown N, Naud C, Mayou D, Li T B, Hass J, Marchenkov A N, Conrad E H, First P N and Heer W A 2006 *Science* **312** 1191

[20] Novoselov K S, Geim A K, Morozov S V, Jiang D, Katsnelson M I, Grigorieva I V, Dubonos S V and Firsov A A 2005 *Nature* **438** 197

[21] Kane C L and Mele E J 2005 *Phys. Rev. Lett.* **95** 226801

[22] Novoselov K S, Jiang Z, Zhang Y, Morozov S V, Stormer H L, Zeitler U, Maan J C, Boebinger G S, Kim P and Geim A K 2007 *Science* **315** 1379

[23] Hui Z X, He P F, Dai Y and Wu A H 2014 *Acta Phys. Sin.* **63** 074401 (in Chinese)

[24] Morpurgo A F and Guinea F 2006 *Phys. Rev. Lett.* **97** 196804

[25] Katsnelson M I 2007 *Materials Today* **10** 20

[26] Geim A K and Novoselov K S 2007 *Nat. Mater.* **6** 183

[27] Tombros N, Jozsa C, Popinciuc M, Jonkman H T and Van Wees B J 2007 *Nature* **448** 571

[28] Sharma S, Kalita G, Ayhan M E, Wakita K, Umeno M and Tanemura M 2013 *Journal of Materials Science* **48** 7036

[29] Yuan L, Liou S H and Wang D 2012 *Phys. Lett. B* **716** 1

[30] Li X, Cai W and An J 2009 *Science* **324** 1312

[31] Huang L, Xu W Y, Que Y D and Mao J H 2013 *Chin. Phys. B* **22** 096803

[32] Khomyakov P A, Giovannetti G, Rusu P C, Brocks G, Brink J van den and Kelly P J 2009 *Phys. Rev. B* **79** 195425

[33] Giovannetti G, Khomyakov P A, Brocks G, Karpan V M, Brink J van den and Kelly P J 2008 *Phys. Rev. Lett.* **101** 026803

[34] Thomas O, Jun Y, Mortensen J J and Thygesem K S 2011 *Phys. Rev. Lett.* **107** 156401

[35] Li B, Chen L and Pan X 2011 *Appl. Phys. Lett.* **98** 133111

[36] Stokbro K 2008 *J. Phys.: Conden. Matter* **20** 064216

[37] Yazyev O V and Pasquarello A 2009 *Phys. Rev. B* **80** 035408

[38] Xia K, Zwierzycki M, Talanana M, Kelly P J and Bauer G E W 2006 *Phys. Rev. B* **73** 064420

[39] Zhou J, Wang L, Qin R, Zheng J, Mei W N and Dowben P A 2011 *The Journal of Physical Chemistry C* **115** 25273